INTERNATIONAL JOURNAL OF OPTIMIZATION IN CIVIL ENGINEERING
Int. J. Optim. Civil Eng., 2019; 9(1):19-37

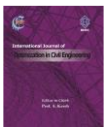

OPTIMAL SMART BASE ISOLATION SYSTEM FOR MULTIPLE EARTHQUAKES

M. Mohebbi[*, †] and H. Dadkhah
Faculty of Engineering, University of Mohaghegh Ardabili, 56199-11367, Ardabil, Iran

ABSTRACT

Hybrid control system composed of a base isolation system and a magneto-rheological damper so-called smart base isolation is one of effective semi-active control system in controlling the seismic response of structures. In this paper, a design method is proposed for designing the smart base isolation system in order to achieve an effective performance under multiple earthquakes. The base mass, the base stiffness and the weighting parameter of H_2/linear quadratic Gaussian control algorithm, which is used to determine the desired control force, have been considered as the design variables and different earthquake records have been considered as design earthquakes. First, the optimum values of these variables under each of the considered earthquakes have been determined by using the genetic algorithm and then, an optimum control system has been designed with multiple earthquakes-based design approach. The defined design objective is minimizing the peak base drift while the peak inter-story drift has been constrained. For numerical simulation, smart base isolation system is designed for controlling a four-story shear frame. The results show that when the control system designed for a specific earthquake is subjected to another earthquake, difference between the performance of this control system and the optimal case under that earthquake is considerable. Hence, the specific earthquake-based design approach is an inappropriate design procedure for smart base isolation. Also, it has been found that control system designed based on multiple earthquakes-based design approach shows effective performance in controlling the response of structure under a wide range of earthquakes.

Keywords: smart base isolation system; magneto-rheological damper; multiple earthquake-based optimum design; genetic algorithm.

Received: 10 February 2018; Accepted: 7 May 2018

[*]Corresponding author: Faculty of Engineering, University of Mohaghegh Ardabili, 56199-11367, Ardabil, Iran
mohebbi@uma.ac.ir (M. Mohebbi)

1. INTRODUCTION

The aim of using different structural control systems in combination together is solving some drawbacks of control systems. Base isolation systems are one of the most effective control systems for controlling the structures against the seismic loadings while the isolated structures mainly experience large drift at the base that can cause serious instabilities in the structure. Different control systems have been employed in combination with the base isolation system in order to solve this drawback and mitigate the base drift. These control systems can be categorized into three types, such as passive [1], semi-active and active [2-4] control systems, based on their adaptability capabilities during the loading. Semi-active control systems are taken into consideration rather than other systems due to capabilities of adaptability and operation with low external supply power. Different semi-active control systems, such as magneto-rheological (MR) damper, variable friction system [5], variable orifice damper [6-8] and piezoelectric friction damper [9], have been studied along the base isolation system.

The most researches conducted in this field have been used MR dampers as supplemental control system [10-13], because these dampers have been commercialized by different companies. MR damper is a semi-active control system which its dynamical properties can be adapted to different conditions by changing the applied voltage [14-16]. The hybrid control system of base isolation and MR damper has been also called smart base isolation (SBI) system. Some of advantages of adding MR damper to the base isolation are achieving a significant reduction in the base drift [17-19] and the capability of adapting both near-field and far-field earthquakes [20]. Increasing the seismic responses of superstructure, such as the inter-story drift and the story acceleration, with respect to passive base isolation (PBI) system without MR damper can be noted as disadvantage of using SBI system [19,21-22].

In order to solve this problem and obtain the best possible design, optimal design of SBI seems necessary. Researches conducted to this end can be classified into two groups based on the considered design variables. In the first group, the studies have focused on optimally designing the control algorithm for the SBI system. Ramallo et al. [18] designed the control algorithm based on try and error for minimizing the base drift with no accompanying increase in the base shear of superstructure. Mohebbi and Dadkhah [23] designed the control algorithm with considering a linear combination of the base drift and acceleration as design objective. In the second group, in addition to the control algorithm, the characteristics of the base isolation system have been also considered as design variables. Mohebbi et al. [24] demonstrated that the characteristics of the base isolation system can significantly affect on the seismic response of structure controlled by the SBI system. They optimally determined both the weighting parameter of control algorithm and the characteristics of the base isolation system while the optimization design problem had been solved for a specific earthquake record.

As noted, the limited studies have been carried out on the optimal design of the SBI system and also in these studies, the effect of earthquake record on the design results has been not considered. Hence in this paper, different earthquake records are considered as design earthquake and first the SBI system is designed optimally for each of the considered earthquakes, separately. Then the inefficiency of the specific earthquake-based design approach is demonstrated under the multiple earthquakes. Finally, a multiple earthquakes-

based optimum design method is proposed for designing the SBI system in order to achieve the best possible design under a wide range of earthquakes.

2. SMART BASE ISOLATION MODEL

SBI has been composed of a base isolation system and a MR damper located at the base. The considered base isolation is mainly a low-damping rubber bearing, which has a linear behavior even until shear strains above 100% [25-26]. Low construction cost and large base drift can be noted as advantage and disadvantage of this system, respectively. Because MR damper effectively reduces the base drift, the low-damping rubber bearing is the best option for combining with MR damper. To simulate this base isolation system, one degree of freedom, which its parameters are dependent of the characteristics of the base isolation, is added to the dynamic model of fixed-base structure. It can be found from the results of previous researches that the structure controlled by SBI system experiences a linear behavior under the seismic loadings. So, it is assumed that the controlled structure has the linear behavior during the seismic loadings. The equation of motion of structure equipped with the SBI system can be written as:

$$M_s\ddot{x}+C_s\dot{x}+K_s x=\Gamma f-M_s\Lambda\ddot{x}_g \tag{1}$$

where M_s, K_s and C_s are the mass, stiffness and damping matrices of system, , x is the displacement vector of the structure relative to the ground, $\Gamma = [-1\ 0]^T$ shows the installed location of MR damper, f is the force applied by MR damper, Λ is a unity vector and $\ddot{x}_g$ is the ground acceleration.

The equation of motion should be rewritten in the state-space form to implement the control algorithm. The rewritten equation can be found in Mohebbi et al. [24], in more detail.

As noted in the SBI system, a MR damper is installed between the base isolation and the ground. MR damper is a semi-active damper which its behavior can be adjusted by changing the applied voltage. The behavior of this damper is strongly nonlinear and the different studies have been conducted to simulate the MR damper behavior [27-30]. Spencer et al. [31] proposed a modified Bouc-Wen model for effectively simulating the MR damper behavior. This modified Bouc-Wen model, which its mechanical model has been shown in Fig. 1, is used for predicting the MR damper force.

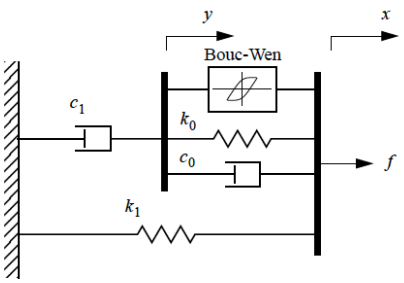

Figure 1. Simple mechanical model of the MR damper

According this model, the applied force is determined as [31]:

$$f = az + c_0(\dot{x} - \dot{y}) + k_0(x - y) + k_1(x - x_0) \tag{2}$$

or equivalently

$$f = c_1\dot{y} + k_1(x - x_0) \tag{3}$$

$$\dot{z} = -\gamma|\dot{x} - \dot{y}|z|z|^{n-1} - \beta(\dot{x} - \dot{y})|z|^n + A(\dot{x} - \dot{y}) \tag{4}$$

$$\dot{y} = \frac{1}{c_1 + c_0}\{az + c_0\dot{x} + k_0(x - y)\} \tag{5}$$

where k_1 and c_1 respectively represent the stiffness and the viscous damping, k_0 and c_0 are respectively present to control the stiffness and the viscous damping at the large velocities, x_0 is the initial displacement of damper, and the parameters n, γ, β and A are used to define the shape of hysteresis loops.

As noted, the MR damper force is dependent of the applied voltage. Spencer et al. [31] presented the following equations to determine the parameters of the modified Bouc-Wen model based on the voltage:

$$a = a(u) = a_a + a_b u \tag{6a}$$

$$c_1 = c_1(u) = c_{1a} + c_{1b}u \tag{6b}$$

$$c_0 = c_0(u) = c_{0a} + c_{0b}u \tag{6c}$$

where u is given as the output of a first-order filter given by:

$$\dot{u} = -\eta(u - V) \tag{7}$$

where V is the voltage and η is a constant modulus.

3. CONTROL ALGORITHM

A control algorithm should be designed to implement the semi-active or active control systems in the adaptive form. H_2/linear quadratic Gaussian (H_2/LQG) controller is a feedback control algorithm, which has been widely used for controlling the semi-active control systems [32-33], and is employed as primary controller in order to determine the desired control force in this paper. Because of the intense nonlinear behavior of MR damper, the voltage can not be determined such that the MR damper force is equaled to the desired control force. On the other hand, the force capacity of MR damper does not permit applying a desired control force more than a specific level. Hence, the utilization of the secondary controller is essential for controlling the SBI system. Clipped-optimal control algorithm is used to make MR damper force track the desired control force. The voltage is determined by this controller at each time step as [34]:

$$V = V_{\max} H\{(f_c - f) f\} \tag{8}$$

V_{max} is the maximum voltage of MR damper, and $H\{.\}$ is the Heaviside step function. According to properties of this function, the voltage is set to zero or V_{max}. f_c is desired control force determined by H_2/LQG control algorithm. In this algorithm, the desired force is obtained by minimizing the following cost function [34]:

$$J = \lim_{\tau \to \infty} \frac{1}{\tau} E[\int_0^{\tau} (z^T(t) Q z(t) + r f_c^2) dt] \tag{9}$$

where Z is the state vector, Q and r are respectively the weighting matrix and the weighting parameter that the desired control force and the performance of SBI are dependent of these weightings. Mohebbi et al. [24] showed the effect of the weighting parameters on the seismic response of structure equipped with the SBI. The researches have been conducted for optimally determining the weighting parameters to control the SBI [18-19,24]. In this paper, the weighting parameters are considered as design variables which will be optimized by the GA.

The correlation between the clipped-optimal and H_2/LQG control algorithms has been shown in Fig. 2. The equations of H_2/LQG controller and parameters defined in this figure have been presented in Mohebbi et al. [24], in more detail.

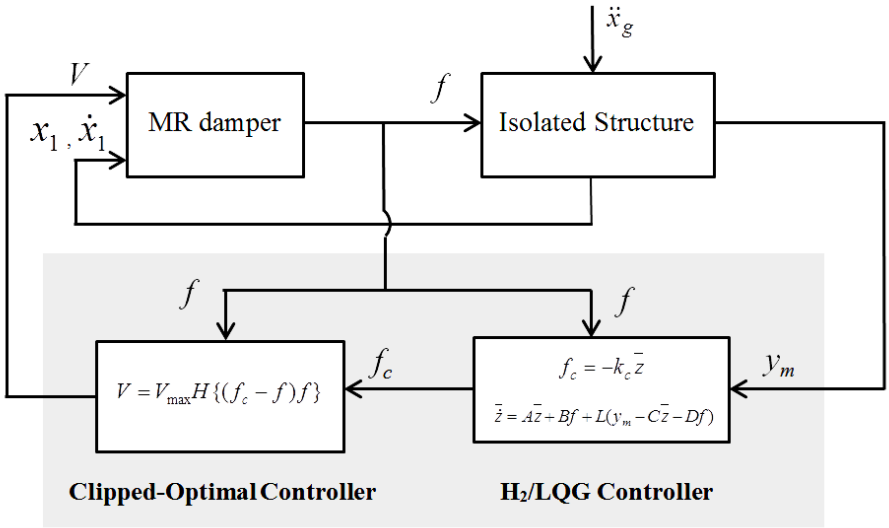

Figure 2. Diagram of clipped-optimal control algorithm

4. OPTIMAL SMART BASE ISOLATION

The structures equipped with the SBI may be subjected under different earthquake records during their life time. Therefore, the effect of different earthquakes should be considered in the design process of SBI in order to achieve the best possible design under multiple

earthquakes. To this end, a multiple earthquakes-based optimum design method is proposed for designing the SBI system. To illustrate the efficiency of proposed design method, the control system has been also designed for each of the considered earthquakes, separately.

4.1 Specific earthquake-based optimum design

In this case, an optimum design problem is defined for designing SBI system under a specific earthquake while the weighting parameter of control algorithm and the characteristics of the base isolation system have been defined as the design variables. Mohebbi et al. [24] demonstrated that the optimum response of structure controlled by SBI system is independent of the weighting matrix Q and only the optimal value of r changes with changing Q. The characteristics of the base isolation system, which can be considered as design variables, are the base mass m_b, the base stiffness k_b and the base damping c_b. Because the low-damping rubber bearing has been used as base isolation system, its damping ratio is defined 2% of the critical damping in the isolated mode and c_b is determined as:

$$c_b = \xi c_{cr} = 0.02 \times 2\sqrt{k_b(m_b + \sum_{i=1}^{n} m_i)} \tag{10}$$

where ξ is the damping ratio, c_{cr} is the critical damping, m_i is the mass of i*th* floor and n is the number of stories.

As noted, MR damper is added to the base isolation system for controlling the base drift while the response of isolated structure may be increased [19,21-22]. Therefore, the design objective is defined minimizing the base drift while a constraint has been applied on the response of superstructure. The seismic response of structure controlled by passive base isolation (PBI) system without MR damper has been considered as the constraint level. Hence, the optimization problem for a specific earthquake can be defined as

Find

$$P = (m_b, k_b, r) \tag{11a}$$

minimize

$$f = \max(d_b) \tag{11b}$$

subject to

$$g_1 = \frac{\max(d_1, d_2, ..., d_n)_{SBI}}{\max(d_1, d_2, ..., d_n)_{PBI}} - 1 \le 0 \tag{11c}$$

where d_b and d_i are the base drift and the inter-story drift of i*th* floor, respectively. As seen, a constraint has been considered for the response of structure such that the maximum inter-story drift of structure controlled by SBI is less that of PBI. In addition to this constraint, m_b

is bounded on interval [$0.7m_f$, $1.3m_f$] where m_f is the floor mass and k_b is constrained such that the fundamental period of the isolated structure has a value on interval [$3T_{fixed}$,3(s)] where T_{fixed} is the fundamental period of the fixed-base structure. These domains of the base mass and the base stiffness have been considered because of the construction limitations and the guidelines proposed by the previous researches and the design codes [35-36].

4.2 Multiple earthquake-based optimum design

In the previous subsection, the optimization design problem was defined for a specific earthquake. In the numerical example section, it will be shown that the result of optimum design is strongly dependent of the considered design earthquake. Hence, the SBI designed for a specific earthquake can not be considered as a well-designed control system for the multiple earthquakes. In this section, a multiple earthquakes-based optimum design method is proposed for the design of SBI in order to achieve the best possible performance under a wide range of earthquakes. In this method, the objective function and the constraint defined in Eq. (11) is developed based on the average of responses under different earthquakes as follow

Find

$$P = (m_b, k_b, r) \tag{12a}$$

minimize

$$f = \sum_{j=1}^{m} \left(\frac{\max(d_b)_{j-SBI}}{\max(d_b)_{j-PBI}} \right) \tag{12b}$$

subject to

$$g_1 = \frac{1}{m} \sum_{j=1}^{m} \frac{\max(d_1, d_2, ..., d_n)_{j-SBI}}{\max(d_1, d_2, ..., d_n)_{j-PBI}} - 1 \le 0 \tag{12c}$$

where m is the number of earthquake records, the subscripts of *j-SBI* and *j-PBI* represent the response of structure controlled by SBI and PBI under j*th* earthquake record, respectively.

For solving the defined optimization problems, GA has been employed and the problems are first formulated as an unconstrained optimization design problem according to the penalty method [37] as:

$$F(V) = \mu f + \beta \max[0, g_1] \tag{13}$$

where μ and β are GA constants that impose the penalty on the constraint of the objective function. Selecting different values for these parameters may affect on the convergence speed of GA runs but has no major effect on the final optimum results [38]. In the defined penalty method, when the maximum inter-story drift of the structure controlled by SBI exceeds that of PBI, g_1 imposes a penalty term to the objective function. In this research, the

parameters of μ and β have been selected as:

$$\mu = 1 \quad and \quad \beta = 10^4 \tag{14}$$

5. GENETIC ALGORITHM

GA is a method for solving the optimization problems that has been developed based on principles inspired by natural genetics [39]. This optimization method has been known as a powerful and robust algorithm in solving the complex and nonlinear optimization problems. Hence, GA has been employed to solve different optimization problems in the structural engineering such as the truss optimization problem [40], optimal design of multiple tuned mass damper [41], stability analysis of gravity dams [42], and optimal locations of the actuators for frame active control [43]. In this paper, the optimum design problems defined in previous section are also solved by GA.

A GA starts with a randomly generated initial population of chromosomes and three different operators are performed to obtain a better chromosome in next generation. Each chromosome can be represented by the real-valued or binary codings that the real-valued coding has been used for chromosome representation in this study. In order to guarantee a better population in the next generation, the elite strategy is applied where a number of the best chromosomes are transferred directly to the next generation. The total number of population in each generation called the population size is important in GA implementation. A low population size may cause inadequate computational accuracy and a high population size will have a large computational cost. A range of 50-150 population size, which is dependent of the number of variables, has been proposed to balance between the accuracy and the computational cost [44]. Because of the existence of three design variables in this study, the population size is set to 50. Basic genetic operators are selection, crossover, and mutation which have been explained briefly.

(1) Selection operator

The selection operator is used to select the chromosomes from the current generation for crossover. The selected chromosomes are considered as parents for generating the next generation. The selection of the chromosomes is mainly performed based on the fitness value of each chromosome. In this study, the fitness value is defined the rank of each chromosome in the sorted objective function and the stochastic universal sampling method [45] has been employed as the selection operator as:

$$P(x_i) = \frac{F(x_i)}{\sum_{i=1}^{N_{ind}} F(x_i)}, i = 1,2,...,N_{ind} \tag{15}$$

where $F(x_i)$ is the fitness value of chromosome x_i, $P(x_i)$ is probability of selection of x_i and N_{ind} is the population size.

(2) Crossover operator

The new chromosomes for the next generation are produced by the crossover operator. In

this paper, the method proposed by Mühlenbein and Schlierkamp-Voosen [46] has been employed as the crossover operator. Two newborns are produced by combining the genes of each pair of parents as follows:

$$O = P_2 + \alpha(P_2 - P_1) \tag{16}$$

where P_1 and P_2 are the genes of parents, O is the newborn gene, and α is a scale factor selected randomly on interval [-0.25,1.25].

(3) Mutation operator

In order to escape from the local optimum, using the mutation operator is essential. This operator generates a newborn with the alteration of the genes of a chromosome. In this study, the Gaussian mutation is used as mutation operator [47] and the mutation ratio, which shows the number of parents selected for mutation, has been selected 4% of the population size.

6. NUMERICAL EXAMPLE

The structure considered for numerical simulations is a four-story shear frame which its properties have been presented in Table 1 [48]. The configuration as well as the matrices of M_s, K_s and C_s of this structure can be found in Mohebbi et al. [24], in more detail.

Table 1: Parameters of structure and base isolation

Story	Floor masses (*ton*)	Stiffness coefficients (*MN/m*)	Damping coefficients (*KN.s/m*)
1	345	340	490
2	345	326	467
3	345	285	410
4	345	250	350

The parameters of modified Bouc-Wen model for MR damper used in this study have been shown in Table 2 [49]. The capacity and the maximum voltage of this damper are 1000 (*kN*) and 10 (*v*), respectively.

Table 1: Modified Bouc-Wen model parameters of MR damper

Parameter	Value	Parameter	Value
c_{0a}	110 *kN.sec/m*	a_a	46.2 *kN/m*
c_{0b}	114.3 *kN.sec/m.V*	a_b	41.2 *kN/m.V*
k_0	0.002 *kN/m*	γ	164 m^{-2}
c_{1a}	8359.2 *kN.sec/m*	β	164 m^{-2}
c_{1b}	7482.9 *kN.sec/m.V*	A	1107.2
k_1	0.0097 *kN/m*	n	2
x_0	0	η	100 sec^{-1}

In this paper, numerical simulations have been performed using the program developed MATLAB software. A comparison between the results of this program and the study of Johnson et al. [17] has been conducted to validate the results of numerical simulations. This validation, which has been presented in Mohebbi et al. [24], shows the acceptable accuracy of the developed program. The numerical simulations of this research are conducted in the following sections:

(a): specific earthquake-based optimum design for SBI

(b): assessment of specific earthquake-based design approach under other earthquakes

(c): multiple earthquakes-based optimum design for SBI

6.1 Specific earthquake-based optimum design for SBI

In this section, five earthquake records, which have been proposed by FEMA P695 [50] and shown in Table 3, have been considered as the design earthquakes and the optimization design problem defined in Eq. (11) is solved for each of these earthquakes using GA.

Table 2: Design earthquake records

Earthquake	M_W	Year	Fault type	Station name	Peak ground acceleration (g)
Duzce, Turkey	7.1	1999	Strike-slip	Bolu	0.73
Hector Mine	7.1	1999	Strike-slip	Hector	0.34
Kobe, Japan	6.9	1995	Strike-slip	Nishi-Akashi	0.50
Superstition Hills	6.5	1987	Strike-slip	Poe Road	0.45
San Fernando	6.6	1971	Thrust	LA - Hollywood Stor FF	0.21

The procedure of solving the optimization problem is explained briefly under Duzce earthquake. For other earthquakes, the solution procedure is quite similar. The operators and characteristics of GA have been defined as explained in section 5. The GA starts with an initial population including 50 randomly generated vectors $P(m_b,k_b,r)$ composed of the base mass, the base stiffness and the weighting parameter. For each vector, the time history analysis of structure is first performed during Duzce earthquake and its responses in terms of the peak inter-story drift and the peak base drift are then determined. Finally, the objective function is calculated for each vector using the penalty method. The vectors, which will be considered as parents for the next generation, are selected using the selection operator for crossover. The crossover operator generates the new vectors by mating the parents. Also in the each generation, a number of the fittest sets (N_{elites}=5) are transferred directly to the next generation as elite and two vectors mutated using the mutation operator are transferred to the next generation. Three different runs of GA with different initial populations are performed in order to ensure the achievement of the global minimum and the accuracy of the optimization procedure. The convergence of the best objective functions in each generation towards an optimum answer for different runs has been shown in Fig. 3. Although the convergence speeds have been different for different funs, almost all runs result the same optimum answer.

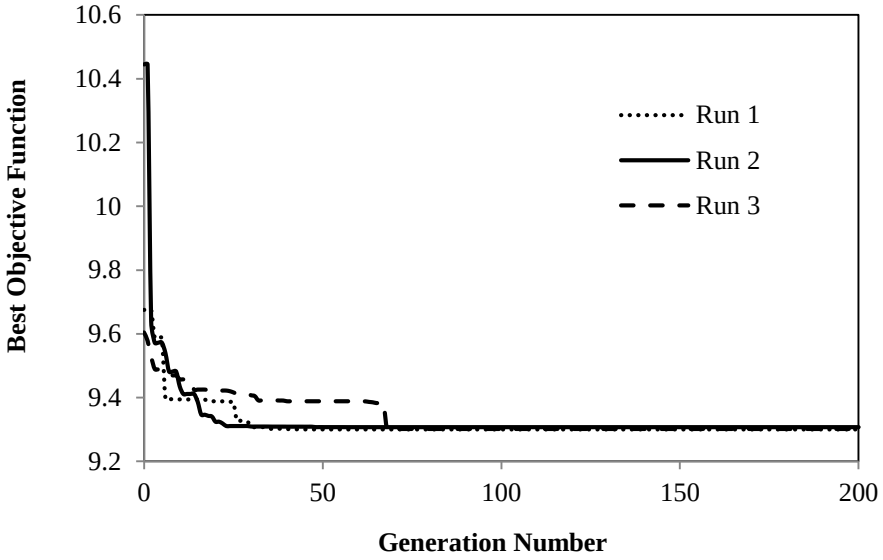

Figure 3. Convergence of the best objective functions towards the optimum answer for three different runs of GA

The optimum design variables have been presented in Table 4 for the considered earthquakes. As shown, the optimum values of design variables are different for each earthquake. Hence, the earthquake record, considered as design earthquake, has significant effect on the optimum design of SBI. The results of optimum designs as well as the peak responses of structure uncontrolled and controlled by PBI have been shown in Table 5. The properties of PBI have been designed according to the guidelines presented in the design codes and previous researches [35-36]. The base mass m_b=345 ton is taken equal to the mass of floor and the base damping c_b is determined using Eq. (10). The base stiffness k_b is designed such that the fundamental period of the isolated structure, which is determined by Eq. (17), is almost triple the fundamental period of the fixed-base structure.

$$T_{iso} = 2\pi\sqrt{\frac{m_b + \sum_{i=1}^{n} m_i}{k_b}} \tag{17}$$

The natural periods of the vibrational modes are equal to 0.60, 0.22, 0.14 and 0.11 s for the fixed-base structure. Hence, the base stiffness k_b=21.3 MN/m is determined by Eq. (17) for T_{iso}=3×0.6=1.8 s.

Table 3: Optimum design variables

Design variables	Duzce, Turkey	Hector Mine	Kobe, Japan	Superstition Hills	San Fernando
m_b (ton)	248.3	240.5	249.5	260.5	246.7
k_b (MN/m)	57.44	71.84	70.51	31.41	11.02
r	1.17E-13	1.91E-14	8.85E-21	1.63E-18	1.71E-19

Table 4: Peak responses of structure uncontrolled and controlled by PBI and optimum SBI

Earthquake	Peak inter-story drift (cm)			Peak base drift (cm)	
	Fixed-base	PBI	Optimum SBI	PBI	Optimum SBI
Duzce, Turkey	8.62	1.93	1.75	36.84	9.30
Hector Mine	2.54	1.59	1.43	31.41	7.29
Kobe, Japan	3.39	1.03	1.03	20.50	4.47
Superstition Hills	3.36	0.66	0.65	11.84	4.79
San Fernando	1.98	0.36	0.36	5.47	3.98

As shown in Table 5, the designed PBI effectively reduces the peak inter-story drift of the fixed-base structure. As instance under Duzce earthquake, a reduction 77.6% in the peak inter-story drift is achieved. In spite of the efficiency of PBI in reducing the inter-story drift, the isolated structure experiences the large drift at the base, especially under strong ground motion records such as Duzce and Hector Mine earthquakes. It can be found from the results that the optimally designed SBI can significantly decrease the peak base drift of structure controlled by PBI. As instance under Duzce and Hector Mine earthquakes, the peak base drifts have been reduced about 74.8% and 76.8%, respectively. Also, the peak inter-story drift of structure controlled by the optimum SBI has no increase with respect to PBI and the constraint defined in the optimization design problem has been satisfied. Therefore, the optimally designed SBI provides a high level of seismic safety in both the structure and the control system.

5.2 Assessment of specific earthquake-based design approach under other earthquakes

In the previous section, the SBI was optimally designed for each of considered earthquakes, separately and the performance of the designed SBI was evaluated under its design earthquake. Because the controlled structures may be subjected to different earthquakes during their life time, the performance of SBI designed for controlling the structure under a specific earthquake is assessed under other earthquakes in this section. As shown in Table 4, five different SBI systems were designed for the considered earthquakes. Each of these designs is evaluated under other earthquakes that the results of this evaluation have been presented in Figs. 4 and 5. These figures demonstrate the peak base drift and inter-story drift of structure controlled by each of SBI systems designed based on a specific earthquake under the considered earthquakes. Also, the peak responses of the structure controlled by PBI have been shown under the considered earthquakes in these figures.

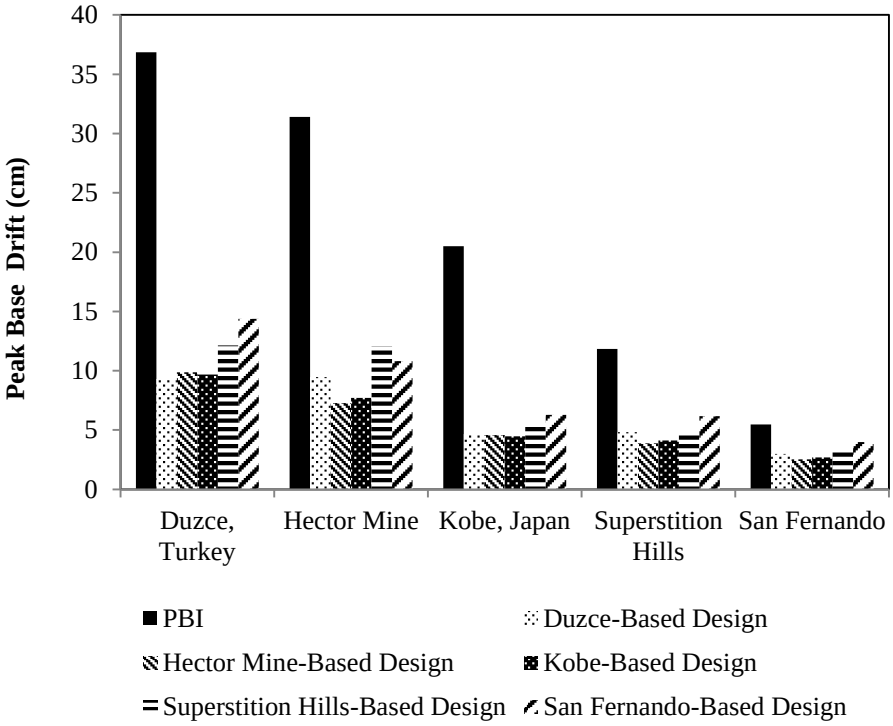

Figure 4. Peak base drift for different specific earthquake-based designs

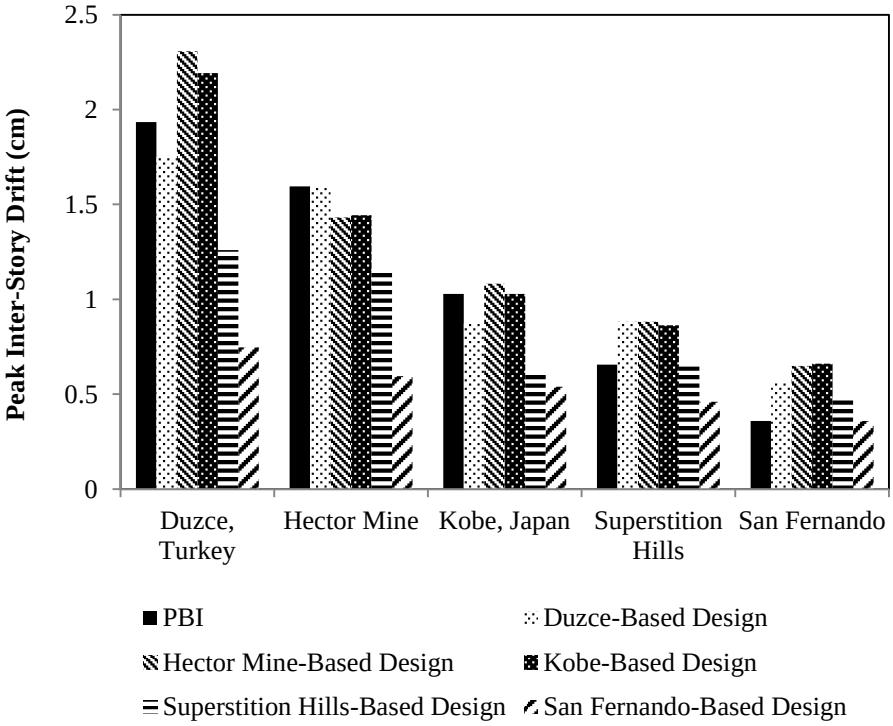

Figure 5. Peak inter-story drift for different specific earthquake-based designs

In the first place, the considerable difference between the performances of different designs can be found according to the results shown in Figs. 4 and 5. As instance under Duzce earthquake, there is a 5.1 cm difference between the performances of SBI systems designed based on the Duzce and San Fernando earthquakes. The comparison between the performances of SBI systems is explained under Duzce and San Fernando earthquakes in more detail while the same results can be found under other earthquakes.

(1) Duzce earthquake: Optimum design for this earthquake, which is the Duzce-based design, gives the minimum peak base drifts as shown in Fig. 4. However, the SBI systems optimally designed based on Hector Mine and Kobe earthquakes also result the peak base drift close to the Duzce-based design. But it can be seen from Fig. 5 that the Hector Mine and Kobe-based designs do not satisfy the constraint defined in the design objective. As instance, when the SBI designed based on Hector Mine earthquake is subjected under Duzce earthquake, there is a 20% increase in the peak inter-story drift with respect to PBI.

(2) San Fernando earthquake: the results of optimum design for this earthquake have been presented by San Fernando-based design as shown in Figs. 4 and 5. From Fig. 4, the SBI systems designed based on other earthquakes give the peak base drift lower than this optimum design. But the peak inter-story drifts of these designs are more than that of PBI and adding MR damper to PBI diminishes the effective performance of PBI. As instance, when the SBI designed based on Kobe earthquake is subjected under San Fernando earthquake, there is a 84% increase in the peak inter-story drift with respect to PBI.

Therefore it can be concluded that a specific earthquake-based design cannot be an appropriate approach for designing SBI and considering the multiple earthquakes is essential in the design procedure.

6.3 multiple earthquakes-based optimum design for SBI

As noted, a multiple earthquakes-based optimum design has been proposed to design an effective SBI under a wide range of earthquakes. To this end, an optimization design problem has been defined based on the average of responses under the multiple earthquakes as explained in section 4.2. In this section, this optimization problem is solved by GA for the considered structure and earthquakes. The optimum values of the design variables determined by GA are m_b=245.7 ton, k_b=40.82 MN/m and r=3.28E-22.

The average of reductions of the structural responses in terms of the peak base drift and the peak inter-story drift under the considered earthquakes has been shown in Figs. 6 and 7 for the multiple earthquakes-based optimum design as well as the specific earthquake-based optimum designs. The negative values presented in Fig. 7 show the increase in the peak inter-story drift with respect to PBI. From the results, the optimum design method proposed based the multiple earthquakes achieves a 62.3% reduction in the peak base drifts averagely under the considered earthquakes while no increase is shown in the peak inter-story drift. Although the Duzce, Hector Mine and Kobe-based designs result more reduction than the multiple earthquakes-based design in the peak base drift, these specific earthquake-based designs are leaded to the increase in the peak inter-story drift with respect to PBI. As instance, a 25.9% increase in the peak inter-story drift with respect to PBI can be seen when the SBI is designed based on Hector Mine earthquake. This increase causes questioning of the main benefit and reason of using the base isolation systems and adding supplemental

MR damper to control base drift can not be justified with the existence of this increase.

Therefore, it can be concluded that under multiple earthquakes, the proposed design method effectively guarantees the achievement of the greatest reduction in the peak base drift with no increase in the peak inter-story drift. Although this objective design may be achieved based on try and error, the main advantage of the proposed design method is its computational efficiency, simplicity as well as being a systematic method.

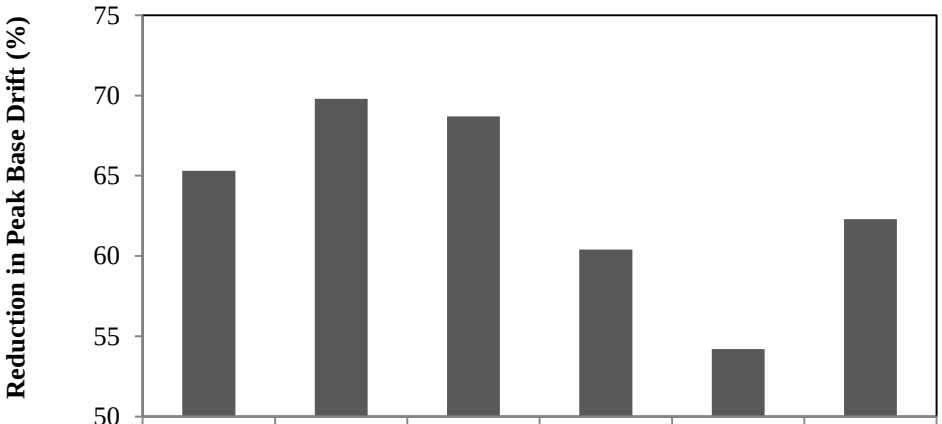

	Duzce-Based Design	Hector Mine-Based Design	Kobe-Based Design	Superstition Hills-Based Design	San Fernando-Based Design	Multiple Eqarthquakes-Based Design
Reduction (%)	65.3	69.8	68.7	60.4	54.2	62.3

Figure 6. Reduction in the peak base drift for specific earthquake and multiple earthquakes-based designs

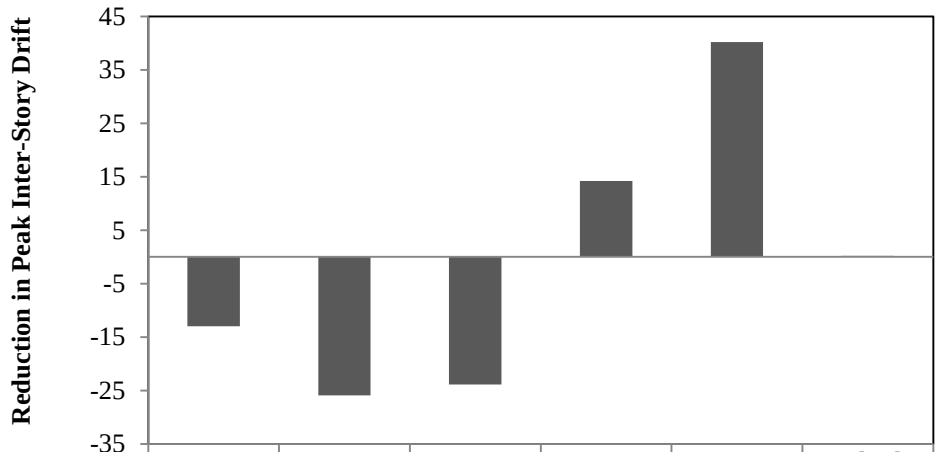

	Duzce-Based Design	Hector Mine-Based Design	Kobe-Based Design	Superstition Hills-Based Design	San Fernando-Based Design	Multiple Eqarthquakes-Based Design
Reduction (%)	-13	-25.9	-23.9	14.2	40.2	0.2

Figure 7. Reduction in the peak inter-story drift for specific earthquake and multiple earthquakes-based designs

7. CONCLUSIONS

In this paper, a multiple earthquakes-based optimum design method has been proposed for designing a smart base isolation system composed of a low-damping rubber bearing and a MR damper. To this end, the design problem has been transformed into an optimization problem which is solved by genetic algorithm. The main characteristics of smart base isolation, such as the base mass, the base stiffness and the weighting parameter defined in the controller, have been considered as design variables and the design objective has been defined minimizing the base drift while the structural response in term of the inter-story drift has been constrained. The reason of applying this constraint is increasing the response of isolated structure when MR damper is added to base isolation for controlling the base drift. For numerical simulation, the smart base isolation is designed for controlling a four-story shear frame. It has been assumed that five earthquake records may be occurred based on the seismic conditions of site and the smart base isolation system is designed under these earthquakes. The control system has been first designed based on specific earthquake-based design approach and the seismic performance of control system designed for a specific earthquake has been then evaluated under other earthquakes. Finally the proposed multiple earthquakes-based optimum design method has been implemented for designing smart base isolation system. The results of specific earthquake-based design approach for different earthquakes show that the optimum values of design variables are strongly dependent on the design earthquake. Hence, the performance of each of the specific earthquake-based designs under other earthquakes has significant difference with respect to the optimal design. As instance, when the control system designed based on San Fernando earthquake is subjected under Duzce earthquake, 55% increase in the peak base drift can be seen with respect to the optimal design for Duzce earthquake. Therefore, the specific earthquake-based design can not be an effective design approach for smart base isolation system. The results of proposed design method based on multiple earthquakes show that this design procedure achieves 62.3% reduction in the peak base drifts averagely under the considered earthquakes while the defined constraint has been satisfied effectively. Therefore, the proposed multiple earthquakes-based optimum design method effectively guarantees the achievement of the maximum reduction in the peak base drift with no increase in the peak inter-story drift.

REFERENCES

1. Constantinou MC, Symans MD, Tsopelas P, Taylor DP. Fluid dampers for application of seismic energy dissipation and seismic isolation, *Proceedings of the ATC-17-1 Seminar on Seismic Isolation, Passive Energy Dissipation and Active Control*, 1999.
2. Inaudi JA, Kelly JM. Hybrid isolation systems for equipment protection, *Earthq Eng Struct Dyn* 1993; **22**(4): 297-313.
3. Yang JN, Wu JC, Reinhorn AM, Riley M. Control of sliding-isolated buildings using sliding-mode control, *J Struct Eng*1996; **122**(2): 179-86.
4. Nagarajaiah S, Riley MA, Reinhorn A. Control of sliding-isolated bridge with absolute acceleration feedback, *J Eng Mech* 1993; **119**(11): 2317-32.
5. Narasimhan S, Nagarajaiah S. Smart base isolated buildings with variable friction systems: H_∞ controller and SAIVF device, *Earthq Eng Struct Dyn* 2006; **35**(8): 921-42.

6. Madden GJ, Symans MD, Wongprasert N. Experimental verification of seismic response of building frame with adaptive sliding base-isolation system, *J Struct Eng* 2002; **128**(8): 1037-45.
7. Wongprasert N, Symans MD. Experimental evaluation of adaptive elastomeric base-isolated structures using variable-orifice fluid dampers, *J Struct Eng* 2005; **131**(6): 867-77.
8. Wongprasert N, Symans MD. Numerical evaluation of adaptive base-isolated structures subjected to earthquake ground motions, *J Eng Mech* 2005; **131**(2): 109-19.
9. Ozbulut OE, Hurlebaus S. Fuzzy control of piezoelectric friction dampers for seismic protection of smart base isolated buildings, *Bull Earthq Eng* 2010; **8**(6):1435-55.
10. Sahasrabudhe S, Nagarajaiah S. Experimental study of sliding base-isolation buildings with magneto-rheological dampers in near-fault earthquake, *J Struct Eng* 2005; **131**(7): 1025-34.
11. Lee HJ, Yang G, Hung HJ, Spencer BF, Lee IW. Semi-active neurocontrol of a base-isolated benchmark structure, *Struct Cont Health Monitor* 2006; **13**(2): 682-92.
12. Zamani AA, Tavakoli S, Etedali S, Sadeghi J. Adaptive fractional order fuzzy proportional - integral - derivative control of smart base-isolated structures equipped with magnetorheological dampers, *J Intell Material Syst Struct* 2017; doi:10.1177/ 1045389X17721046.
13. Mohebbi M, Dadkhah H. Performance of Semi-Active Base Isolation Systems under External Explosion, *Int J Str Stab Dyn* 2017; **17**(10): 1750112.
14. Moon SJ, Huh YC, Jung HJ, Jang DD, Lee HJ. Sub-optimal design procedure of valve-mode magnetorheological fluid dampers for structural control, *KSCE J Civil Eng* 2011; **15**(5): 867-73.
15. Cho SW, Jung HJ, Lee IW. Smart passive system based on magnetorheological damper, *Smart Mater Struct* 2005; **14**(4): 707-14.
16. Zabihi-Samani M, Ghanooni-Bagha M. An optimal cuckoo search-fuzzy logic controller for optimal structural control, *Int J Optim Civil Eng* 2018; **8**(1): 117-35.
17. Johnson EA, Ramallo JC, Spencer BF, Sain MK. Intelligent base isolation systems, *Proceedings of the 2nd World Conference on Structural Control* 1999, Kyoto, Japan; **1**: pp. 367-376.
18. Ramallo JC, Johnson EA, Spencer BF, Smart base isolation systems, *J Eng Mech* 2002; **128**(10): 1088-99.
19. Mohebbi M, Dadkhah H, Shakeri K. Optimal hybrid base isolation and MR damper, *Int J Optim Civil Eng* 2015; **5**(4): 493-509.
20. Yoshioka H, Ramallo JC, Spencer BF. Smart base isolation strategies employing magnetorheological dampers, *J Eng Mech* 2002; **128**(5): 540-51.
21. Spencer BF, Johnson EA, Ramallo JC. Smart isolation for seismic control, *JSME Int J Ser C* 2000; **43**(3): 704-11.
22. Ali SF, Ramaswamy A. Hybrid structural control using magnetorheological dampers for base isolated structures, *Smart Mater Struct* 2009; **18**(5): 055011.
23. Mohebbi M, Dadkhah H. Multi-objective semi-active base isolation system, *Int J Optim Civil Eng* 2017; **7**(3): 319-38.
24. Mohebbi M, Dadkhah H, Dabbagh HR. A genetic algorithm–based design approach for smart base isolation systems, *J Intell Material Syst Struct* 2017; doi: 10.1177/ 1045389X17733058.
25. Naeim F, Kelly JM. *Design of seismic isolated structure: from theory to practice*, John Wiley & Sons, New York, 1999.

26. Vu DC, Politopoulos I, Diop S. A new semi-active control based on nonlinear inhomogeneous optimal control for mixed base isolation, *Struct Cont Health Monitor* 2018; **25**(1): e2030.
27. Li WH, Yao GZ, Chen G, Yeo SH, Yap FF. Testing and steady state modeling of a linear MR damper under sinusoidal loading, *Smart Mater Struct* 2000; **9**(1): 95-102.
28. Snyder RA, Kamath GM, Wereley NM. Characterization and analysis of magnetorheological damper behavior under sinusoidal loading, *AIAA J* 2001; **39**(7): 1240-53.
29. Xia PQ. An inverse model of MR damper using optimal neural network and system identification, *J Sound Vib* 2003; **266**(5): 1009-23.
30. Wang DH, Liao WH. Magnetorheological fluid dampers: a review of parametric modelling, *Smart Mater Struct* 2011; **20**(2): 023001.
31. Spencer BF, Dyke SJ, Sain MK, Carlson JD. Phenomenological model for magnetorheological dampers, *J Eng Mech* 1997; **123**(3): 230-8.
32. Nagarajaiah S, Narasimhan S. Smart base-isolated benchmark building. Part II: phase I sample controllers for linear isolation systems, *Struct Cont Health Monitor* 2006; **13**(2-3): 589-604.
33. Fallah FY, Taghikhany T. Time-delayed decentralized H_2/LQG controller for cable-stayed bridge under seismic loading, *Struct Cont Health Monitor* 2013; **20**(3): 354-72.
34. Dyke SJ, Spencer BF, Sain MK, Carlson JD. Modeling and control of magnetorheological dampers for seismic response reduction, *Smart Mater Struct* 1996; **5**(5): 565-75.
35. Villaverde R. *Fundamental Concepts of Earthquake Engineering*, Taylor and Francis group, New York, 2009.
36. Bisch P, Carvalho E, Degee H, Fajfar P, Fardis M, Franchin P, Kreslin M, Pecker A, Pinto P, Plumier A, Somja H, Tsionis G. *Eurocode 8: Seismic Design of Buildings Worked Examples*, JRC technical report, Publications Office of the European Union/Joint Research Centre, Luxembourg, 2012.
37. Rao SS. *Engineering Optimization: Theory and Practice*, John Wiley & Sons, New Jersey, 2009.
38. Joghataie A, Mohebbi M. Vibration controller design for confined masonry walls by distributed genetic algorithms, *J Struct Eng* 2008; **134**(2): 300-9.
39. Holland JH. *Adaptation in Natural and Artificial Systems*, The MIT Press Cambridge, London, 1975.
40. Salar M, Ghasemi MR, Dizangian B. A fast GA-based method for solving truss optimization problems, *Int J Optim Civil Eng* 2016; **6**(1): 101-14.
41. Mohebbi M. Minimizing Hankel's norm as design criterion of multiple tuned mass dampers, *Int J Optim Civil Eng* 2013; **3**(2): 271-88.
42. Haghighi A, Ayati AH. Uncertainty analysis of stability of gravity dams using the fuzzy set theory, *Int J Optim Civil Eng* 2015; **5**(4): 465-78.
43. Rezaiee-Pajand M, Payandeh Sani M. Three schemes for active control of the planar frame, *Int J Optim Civil Eng* 2015; **5**(1): 117-35.
44. Pham DT, Karaboga D. *Intelligent Optimisation Techniques: Genetic Algorithms, Tabu Search, Simulated Annealing and Neural Networks*, Springer, London, 2012.
45. Baker JE. Reducing bias and inefficiency in the selection algorithm, *Proceedings of the 2nd International Conference on Genetic Algorithm (ICGA), Cambridge, MA, USA* 1987; pp. 14-21.

46. Muhlenbein H, Schlierkamp-Voosen D. Predictive models for the breeder genetic algorithm: I. continuous parameter optimization, *Evolut Comput* 1993; **1**(1): 25-49.
47. Dong H, He J, Huang H, Hou W. Evolutionary programming using a mixed mutation strategy, *Inform Sci* 2007; **177**(1): 312-27.
48. GÜÇLÜ R. Fuzzy logic control of vibrations of analytical multi-degree-of-freedom structural systems, *Turkish J Eng Environ Sci* 2003; **27**(3): 157-68.
49. Jung HJ, Spencer BF, Lee IW. Control of seismically excited cable-stayed bridge employing magnetorheological fluid dampers, *J Struct Eng* 2003; **129**(7): 873-83.
50. FEMA P695. *Quantification of Building Seismic Performance Factors*, Federal Emergency Management Agency, Washington, DC, 2009.